Int J Adv Manuf Technol
DOI 10.1007/s00170-013-5004-z

ORIGINAL ARTICLE

Mathematical model for cutting force in rotary ultrasonic face milling of brittle materials

Chenglong Zhang · Jianfu Zhang · Pingfa Feng

Received: 6 December 2012 / Accepted: 8 April 2013

Abstract Rotary ultrasonic machining of brittle materials, such as glass, ceramics, silicon, and sapphire, has been explored in a large number of experimental and theoretical investigations. Mechanistic models have been developed to predict the material removal rate or cutting force in the rotary ultrasonic machining of brittle materials. However, most merely describe the rotary ultrasonic machining process of drilling holes in brittle materials. There are no reports on the development of a cutting force model for flat surface rotary ultrasonic machining, i.e., rotary ultrasonic face milling. This paper presents a mathematical model for the cutting force in the rotary ultrasonic face milling of brittle materials under the assumption that brittle fracture removal is the primary mode of material removal. Verification experiments are conducted for the developed cutting force model and show that the trends of input variables for the cutting force agree well with the trends of the developed cutting force model. The developed cutting force model can be applied to evaluate the cutting force in the rotary ultrasonic face milling of brittle materials.

Keywords Rotary ultrasonic machining · Face milling · Mathematical model · Cutting force · Brittle material

C. Zhang · J. Zhang · P. Feng
The State Key Laboratory of Tribology,
Department of Mechanical Engineering,
Tsinghua University, Beijing 100084, China

J. Zhang
e-mail: zhjf@tsinghua.edu.cn

P. Feng
e-mail: fengpf@mail.tsinghua.edu.cn

C. Zhang (✉) · J. Zhang · P. Feng
Institute of Manufacturing Engineering,
Department of Mechanical Engineering,
Tsinghua University, Room 2502(9003 Building),
Beijing 100084, People's Republic of China
e-mail: zcl08@mails.tsinghua.edu.cn

1 Introduction

Brittle materials such as optical glass and engineering ceramics have been widely used in many fields, such as optics, electronics, semiconductors, and aerospace, owing to their superior physical, mechanical, optical, or electronic properties (e.g., high hardness, high strength, high wear resistance, and chemical stability) [1–4]. There is a demand to manufacture precision parts made from such materials. However, because of their high hardness and low fracture toughness, brittle materials are considered difficult to machine. Manufacturing of such materials has become a rigorous task [5]. In the last two decades, various machining technologies of brittle materials have been developed and made available, such as cutting [6], grinding [7], drilling [8], and lapping [9]. In addition, some nontraditional machining processes have been successfully applied to the processing of brittle materials, such as electrolytic in-process dressing grinding [10], abrasive water jet machining [11], ultrasonic machining [12, 13], ultrasonic vibration-assisted cutting [14–16], two-dimensional ultrasonic vibration-assisted grinding [17–19], ultrasonic vibration-assisted milling [20, 21], and rotary ultrasonic machining (RUM) [22–24].

As a nontraditional machining process, RUM is a hybrid process that combines the material removal mechanism of diamond grinding and ultrasonic machining [25]. Since its birth in the 1960s, RUM has been used in the machining of many types of brittle materials such as glass [23, 26], engineering ceramic [2], silicon [27], and ceramic matrix composite [25]. Figure 1 illustrates the RUM process, where D_o is the diamond tool outer diameter, and D_i is the diamond tool inner diameter. A rotating tool with metal-bonded diamond abrasives is ultrasonically vibrated in the axial direction and feeds towards the workpiece at a constant feed rate. The motion of the diamond particle or the tip of the diamond tool is a combination of the rotational motion of the spindle, ultrasonic

Published online: 27 April 2013

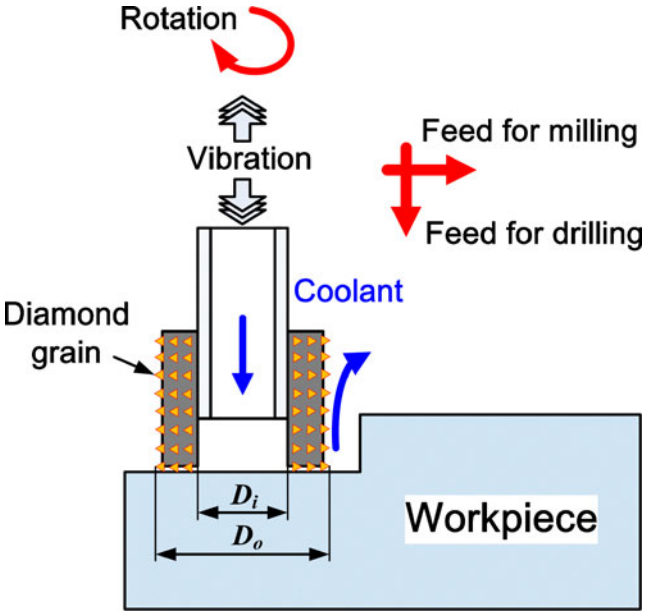

Fig. 1 Illustration of the RUM [24]

vibration, and feed of the diamond tool. The machining process becomes milling as the feed direction of the tool becomes perpendicular to the direction of ultrasonic vibration, and becomes drilling as the feed direction of the tool becomes parallel to the direction of ultrasonic vibration [28].

A review of existing reports shows that, compared with traditional machining, RUM has many advantages, such as smaller cutting force, smaller chipping size, less subsurface damage, and less tool wear. There are many experimental and theoretical research reports on RUM, but few reports in the literature on models of RUM, namely the material removal rate model [2, 29, 30] and cutting force model [31, 32]. Additionally, the material removal rate and tool wear rate in ultrasonic machining have been mathematically modeled [33, 34]. However, the developed cutting force models merely describe the process of drilling holes. At present, there is no cutting force model for flat surface RUM, i.e., rotary ultrasonic face milling (RUFM).

Some studies have found RUFM to be workable for the machining of brittle materials such as optical glass and ceramics [26, 35, 36]. Moreover, the cutting force is known as a characteristic of the machining process and has been applied to clarify the cutting process since it directly affects tool wear, cutting temperature, residual stress, and surface integrity [37]. Therefore, the development of the cutting force model for the RUFM of brittle materials is desirable to help predict machining performance and optimize input variables.

In this paper, a mathematical model is developed to predict the cutting force in the RUFM of brittle materials according to the material brittle fracture removal mechanism. The main approach to develop the cutting force model began with an analysis of a single abrasive particle considered as the basic component of cutting forces induced in diamond cutter machining, and then, the model was derived by summing the forces on all particles taking part in cutting, which has been presented in a great many publications for the cutting force modeling of many abrasive machining scenarios [31, 32, 38].

In the modeling of the cutting force, the effective processing time, processing depth, processing speed, and processing length of a single grit in RUFM are also determined through the analysis of material removal mechanisms of RUFM, i.e., a combination of grinding and ultrasonic machining. After the development of the cutting force model, the proportionality parameter for optical glass (K9) is obtained through designed experiments and calculations. The developed cutting force model is then verified in pilot experiments. Conclusions are drawn in the final section.

2 Material removal characteristics of brittle materials in RUFM

2.1 Kinematics characteristics of an abrasive particle in RUFM

RUFM can be regarded as a combination of diamond grinding and tool ultrasonically vibrated machining. The motion of diamond grit in RUFM is a combination of rotational motion, ultrasonic vibration in the direction of the tool axis, and horizontal feed motion, as shown in Fig. 1. Therefore, the motion trajectory of diamond grit in RUFM can be expressed as

$$S_{RUFM}(t) = \begin{bmatrix} r \cdot \sin(\omega t) + v_{cx} \cdot t \\ r \cdot \cos(\omega t) + v_{cy} \cdot t \\ A \cdot \sin(2\pi f t) \end{bmatrix}, \tag{1}$$

where r is the rotational radius of the diamond particle, A is the ultrasonic vibration amplitude, f is the ultrasonic vibration frequency, ω is the angular velocity of the diamond particle, v_{cx} and v_{cy} are the feed rates in the x-axis and y-axis directions, respectively, and t is the processing time.

According to Eq. (1), the hybrid velocity of the diamond particle can be described as

$$v_{RUFM} = \frac{dS_{RUFM}(t)}{dt} = \begin{bmatrix} r \cdot \omega \cos(\omega t) + v_{cx} \\ -r \cdot \omega \sin(\omega t) + v_{cy} \\ 2\pi f A \cdot \cos(2\pi f t) \end{bmatrix}. \tag{2}$$

The acceleration of the diamond particle in RUFM can be then derived from Eq. (2) as

$$a_{RUFM} = \frac{dv_{RUFM}(t)}{dt} = \begin{bmatrix} -r \cdot \omega^2 \sin(\omega t) \\ -r \cdot \omega^2 \cos(\omega t) \\ -4\pi^2 f^2 A \cdot \sin(2\pi f t) \end{bmatrix}. \tag{3}$$

Figure 2 shows the trajectory of one diamond particle and the kinematic characteristics of the diamond particle in

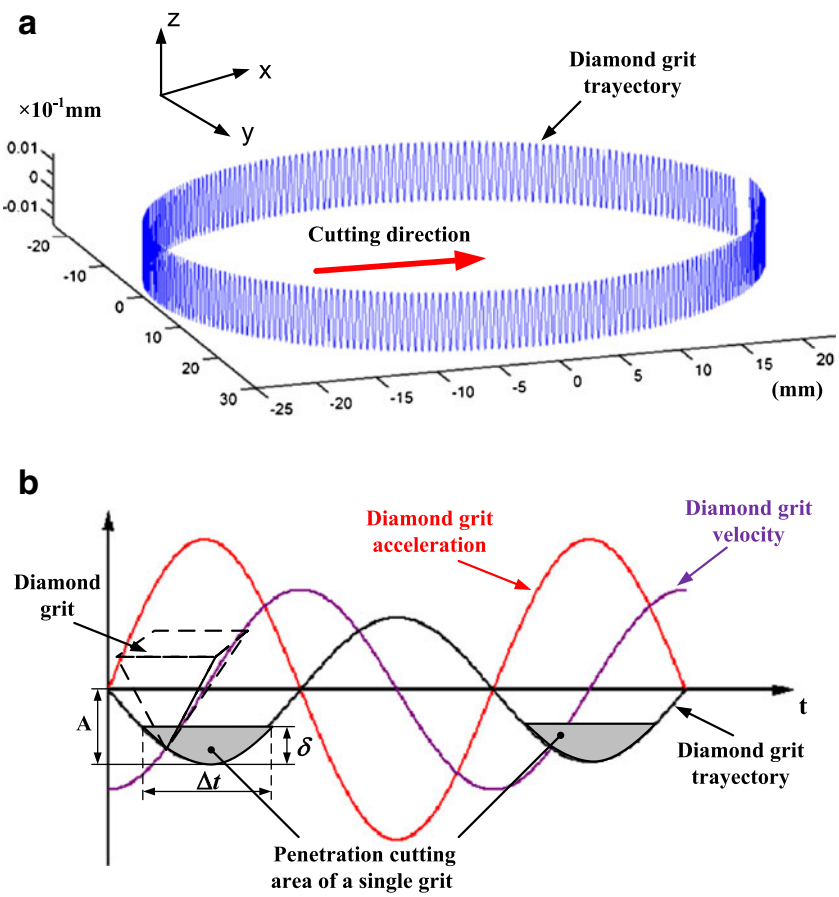

Fig. 2 **a** Trajectory of a diamond particle in RUFM. **b** Kinematic characteristics of the diamond particle in RUFM

RUFM, where Δt is the period of time that the particle is in contact with the workpiece (i.e., the effective cutting time), and δ is the maximum cutting depth that an abrasive particle penetrates into the workpiece. Figure 2a is drawn for the initial values r=25 mm, ω=4,000 rad/min, f=10 kHz, and A= 10 μm. Figure 2b is obtained from Eqs. (1), (2), and (3).

Figure 2b shows that, owing to the ultrasonic vibration of the diamond tool, the cutting process of the diamond particle sintered on the end face of the tool is interrupted instead of there being continuous contact with the workpiece. In each vibration cycle, the diamond particle on the end face of the diamond tool penetrates into the workpiece for a certain period of time, which is called the effective cutting time Δt, and the actual cutting depth of the abrasive particle is the period change, as shown in Fig. 2b. The calculations of the effective cutting time Δt and maximum cutting depth δ will be presented later as they are needed.

2.2 Material removal of brittle materials in RUFM

During the diamond tool processing of brittle materials, the shape of the diamond particles sintered on the end face of the tool is generally irregular and has many sharp corners. The diamond particles acting on the workpiece surface behave in many ways just like indenters. Existing research has shown that there are two material removal modes in the machining of hard and brittle materials, namely the brittle fracture mode and ductile mode, and indentation and scratch processes have been applied to reveal the material removal of brittle materials during diamond processing [39, 40]. In the RUM of brittle materials, existing reports have shown that there are also a brittle fracture mode and ductile mode [2]. In this study, the mathematical cutting force model is presented under the assumption that the material removal mode of brittle materials in RUFM is totally brittle fracture.

In the machining of brittle materials in RUFM, median–radial cracks and lateral cracks are generated while diamond particles are indented into the workpiece surface. The initiation and propagation of these radial and lateral cracks, in the end, cause the chipping of the workpiece, which leads to material removal in brittle mode. Figure 3 shows the material removal of brittle materials and the volume calculation in the brittle fracture mode processed by an abrasive particle, where C_m is the depth of the median crack from the unmachined surface, C_L is the length of the lateral crack, C_h is the depth of the lateral crack, and α_0 is the apex angle of the abrasive grain.

In the RUFM of brittle materials, abrasive particles remove the material on the workpiece surface through diamond particle machining induced by diamond tool rotary,

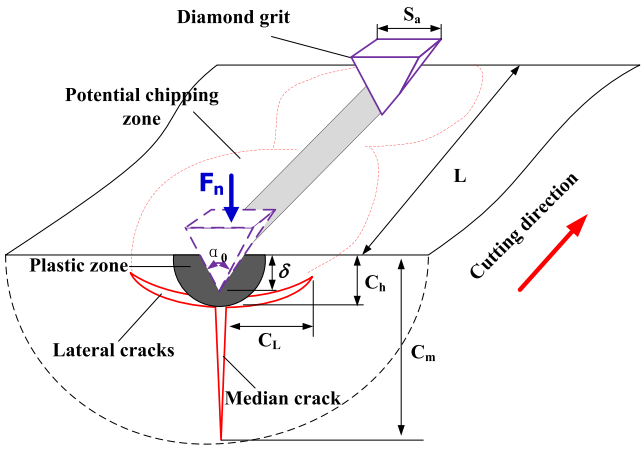

Fig. 3 Schematic diagram of material removal and volume calculation in brittle fracture mode induced by the abrasive particle process

ultrasonic impact, and hybridizing abrasion with impact due to ultrasonic vibration. Therefore, the material removal volume processed by one diamond particle during a single vibration cycle can be determined by the lateral crack length and depth and the distance of the particle contact with the workpiece in a vibration cycle. To simplify the calculation of the volume of material removal, the actual volume of material removal induced by a diamond particle is defined as being proportional to the theoretical volume of the fracture removal zone during a vibration cycle in this paper. Thus, the material removal volume V of one diamond particle in a vibration cycle can be expressed as

$$V = 2K \cdot C_L \cdot C_h \cdot L, \tag{4}$$

where K is a proportionality parameter that can be obtained via designed experiments for a given workpiece material, and L is the effective cutting length of an abrasive particle with effective cutting time Δt. The calculations of effective cutting length L, lateral crack length C_L, and lateral crack depth C_h are presented in a later section.

3 Development of a cutting force model

For the development of a cutting force model, some major assumptions and simplifications are used in this study.

1. Diamond particles taking part in the cutting process are rigid octahedrons of the same size because the shape of diamond particles sintered on the end of diamond tool has many sharp corners, and each diamond particle acts on the workpiece surface like a Vickers indenter.
2. During each ultrasonic vibration cycle, diamond particles located on the tool end surface have the same height and all take part in cutting.
3. The workpiece material is an ideally brittle material. All the removed material on the workpiece surface is in brittle fracture mode suitable for the brittle fracture removal mechanism.

The modeling of the cutting force in this paper is organized into three main steps. The first step is to investigate the interaction between the individual diamond particle and the workpiece and establish the relationship between the cutting force and maximum penetration depth of the diamond particle. The relation for the volume of material removal induced by one diamond particle in a single vibration cycle is then presented. Finally, the cutting force model is derived by aggregating the effects of all the working diamond particles in the RUFM process.

To facilitate the modeling process, possible input variables are defined and denoted by the symbols given in Table 1.

In RUFM, the motions of diamond particles are considered as sinusoidal with amplitude A and frequency f owing to their oscillatory nature. The position of each diamond particle in the z direction relative to its mean position can be expressed as Eq. (1). Figure 2b shows that the diamond abrasive particle on the end face of the diamond tool is not in continuous contact with the workpiece. The certain period of time that the diamond particle effectively processes the workpiece surface in a single ultrasonic vibration cycle is called the effective cutting time Δt. It takes a diamond particle $\Delta t/2$ to move from $y=(A-\delta)$ to $y=A$. Therefore, Δt can be accurately calculated as

$$\Delta t = \frac{1}{\pi f}\left[\frac{\pi}{2} - \arcsin\left(1 - \frac{\delta}{A}\right)\right], \tag{5}$$

where Δt is the period of time during which the particle is in contact with the workpiece, A is the ultrasonic vibration amplitude, f is the ultrasonic vibration frequency, and δ is the maximum penetration depth.

The maximum depth δ of a single abrasive particle penetrating into the workpiece (see Fig. 2b), according to the indentation fracture mechanics mechanism, can be calculated as [41]

$$F_0 = \frac{1}{2}\xi\delta^2 \tan(\alpha_0/2)H_v, \tag{6}$$

where F_0 is the maximum contact force acting on the workpiece for one diamond particle, in newton; H_v is the hardness of the workpiece material, in megapascal; and ξ is the geometrical factor of the indenter (defined as 1.85 in paper [41]). F_0 can then be obtained as

$$F_0 = \frac{F_c}{m}, \tag{7}$$

where F_c is the maximum impact force between the diamond tool and workpiece, in newton, and m is the number of diamond particles taking part in the cutting. The definition of abrasive concentration can be applied to calculate the number of diamond abrasive particles on the end of the diamond tool, which

Table 1 Input variables in the development of a cutting force model for RUFM

Input variables	Definitions and symbols	Unit
Diamond tool variables	1. Diamond tool outer diameter, D_o	mm
	2. Diamond tool inner diameter, D_i	mm
	3. Abrasive concentration, C_a	Dimensionless
	4. Abrasive size, S_a	mm
Workpiece material properties	5. Elastic modulus, E	MPa
	6. Poisson's ratio, ν	Dimensionless
	7. Fracture toughness, K_{IC}	MPa $m^{1/2}$
	8. Hardness, H_v	MPa
Ultrasonic vibration variables	9. Amplitude, A	μm
	10. Frequency, f	Hz
Machining process variables	11. Feed rate, v_c	mm/min
	12. Spindle speed, n	rpm
	13. Cutting depth, d_c	mm
	14. Cutting width, w_c	mm

has been described in detail in the literature [31]. The number of active abrasive particles on the end face of the diamond tool can be obtained as

$$m = C_1 \frac{C_a^{2/3} A_0}{S_a^2}, \tag{8}$$

where C_a is the abrasive concentration; S_a is the abrasive size, in millimeter, as shown in Fig. 3; A_0 is the area of the core drill end face, $A_0=\pi(D_o{}^2-D_i{}^2)/4$, in square millimeter; D_o and D_i are the outer and inner diameters of the diamond tool, respectively, in millimeter, as shown in Fig. 1; and C_1 is a dimensionless constant.

Since it is assumed that the diamond grains are incompressible, the impulse I_1 in terms of the maximum contact force F_c during one ultrasonic vibration cycle is

$$I_1 = \int_T F_c dt \approx F_c \cdot \Delta t. \tag{9}$$

The impulse (I_2) for one ultrasonic vibration cycle in terms of the cutting force F is

$$I_2 = F \cdot \frac{1}{f} = \frac{F}{f}, \tag{10}$$

where F is the cutting force measured in the RUFM of brittle materials. The cutting force F measured in the RUFM is different from the maximum impact force F_c. The relationship between F and F_c can be obtained by equating the impulse in terms of F_c to the impulse in terms of F during each vibration cycle. By equating the two impulses I_1 and I_2, we get

$$F_c \cdot \Delta t = \frac{F}{f}. \tag{11}$$

Substituting Eq. (7) into Eq. (11), the relationship between F and F_0 is derived as

$$F = m \cdot f \cdot F_0 \cdot \Delta t. \tag{12}$$

As shown in Fig. 3, L is the effective cutting length of an abrasive particle with effective cutting time Δt. It is determined by the hybrid velocity of the diamond particle and effective cutting time Δt, which can be calculated by

$$\begin{aligned} L &= \int_{t_1}^{t_2} V_{RUFM} dt \\ &= \int_{t_1}^{t_2} \sqrt{r^2 \cdot \omega^2 + V_x^2 + V_y^2 + 2 \cdot V_x \cdot r \cdot \omega \cos(\omega t) - 2 \cdot V_y \cdot r \cdot \omega \sin(\omega t)} dt, \end{aligned} \tag{13}$$

where r is the rotating radius of the diamond particle, taken as $(D_o+D_i)/2$, in millimeter, and n is the spindle speed, revolution per minute.

Since

$$\begin{aligned} &v_{cy} \ll r \cdot \omega, \\ &\Delta t = t_2 - t_1, \\ &v_{cx} = 0, \end{aligned}$$

it follows that

$$L = \int_{t_1}^{t_2} V_{RUFM} dt \approx r \cdot \omega \cdot \Delta t = \frac{2\pi n r}{60} \cdot \Delta t. \tag{14}$$

The diamond particles acting on the workpiece surface behave in many ways just like indenters in RUFM. Therefore, the particle will generate median–radial cracks and lateral cracks in the workpiece surface according to

indentation fracture mechanics during the material removal. For the length of the lateral crack C_L and the depth of the lateral crack C_h, we have [42]

$$C_L = k_1 \cdot \left(\cot\frac{\alpha_0}{2}\right)^{5/12} \cdot \left(\frac{E^{3/4}}{H_v \cdot K_{IC} \cdot (1-\nu^2)^{1/2}}\right)^{\frac{1}{2}} \cdot (F_0)^{\frac{5}{8}}, \tag{15}$$

$$C_h = k_2 \cdot \left(\cot\frac{\alpha_0}{2}\right)^{1/3} \cdot \frac{E^{1/2}}{H_v} \cdot (F_0)^{\frac{1}{2}}, \tag{16}$$

where C_L is the lateral crack length, in millimeter; C_h is the lateral crack depth, in millimeter; K_{IC} is the fracture toughness of the workpiece material, in megapascal meter$^{1/2}$; E is the elastic modulus of the workpiece material, in megapascal; ν is Poisson's ratio of the workpiece material; and k_1 and k_2 are the dimensionless constants, which are dependent on the material/indenter system.

According to the relation presented for the material removal volume V of one diamond particle in a vibration cycle (i.e., Eq. (4)), the material removal rate of one diamond particle can be described as

$$MRR_0 = f \cdot V = 2K \cdot C_L \cdot C_h \cdot L \cdot f. \tag{17}$$

The material removal rate of the diamond tool can be derived by the summation of MRR_0 for all particles active on the end of the diamond tool. Thus, the material removal rate for the rotary ultrasonic face milling of brittle materials in brittle fracture removal mode (MRR_D) can be obtained from

$$MRR_D = 2K \cdot m \cdot C_L \cdot C_h \cdot L \cdot f. \tag{18}$$

In addition, MRR_D can also be calculated in terms of the process parameters, including feed rate, cutting depth, and cutting width:

$$MRR_D = v_c \cdot w_c \cdot d_c, \tag{19}$$

where v_c is the feed rate of the cutting tool, in millimeter per second; w_c is the cutting width, in millimeter; and d_c is the cutting depth, in millimeter.

To simplify the numerical computation, we simplify the equation for the contact time Δt as

$$\Delta t = \frac{\delta}{2Af}. \tag{20}$$

By substituting Eqs. (6), (8), (12), (14), (15), (16), and (20) into Eq. (18), and equating Eqs. (18) and (19), we obtain the relationship between cutting force F and input variables:

$$F = K \cdot \left[\frac{H_v^{35} \cdot K_{IC}^{12} \cdot (1-\nu^2)^6 \cdot C_a^{4/3} \cdot v_c^{24} \cdot w_c^{24} \cdot d_c^{24} \cdot (D_o - D_i)^2}{\xi \cdot \cot^{17}(\alpha_0/2) \cdot E^{21} \cdot S_a^4 \cdot A^2 \cdot n^{24} \cdot (D_o + D_i)^{22}}\right]^{1/26}, \tag{21}$$

where K is a proportionality constant that is the correction factor of the cutting force. The value K can be obtained from experiments on the RUFM of hard–brittle materials.

4 Obtaining the proportionality constant K

4.1 Experimental setup

Rotary ultrasonic face milling experiments were conducted on a rotary ultrasonic machine (DMG Ultrasonic 50, DMG, Germany). The machine mainly consists of an ultrasonic spindle system, a numerical control machining system, and a coolant system. The maximum power of the rotary ultrasonic machine is 300 W and the maximum ultrasonic machining spindle speed is 8,000 rpm. In this study, a galvanic coated diamond milling cutter is used. During this binding type of the tool, the binding on the basic material body is isolated from the steel in an electronic–galvanic way, which leads to a grinding layer with big chip space volume. The outer diameter of the diamond tool is 10 mm with wall thickness of 1 mm, and diamond particle size (mesh) of D91. Processing fluid (Blaser, Switzerland) was used as internal coolant and external coolant.

A Kistler 9256C2 dynamometer (Kistler Instrument Corp, Switzerland) was used to record the cutting forces along the normal direction during the experiments. The signal from the dynamometer was passed through an amplifier (5070A). The amplified signal was fed to a data recorder (2855A4). The recorded data were downloaded onto a personal computer. The sampling frequency was 5 kHz. The average value of the cutting force, which is the mean value of the entire cutting force curve, was chosen to represent the cutting force.

4.2 Design of experiments

The workpiece was K9 optical glass. Mechanical properties of the workpiece material were obtained in indentation tests: elastic modulus E=85.9 GPa, hardness H_v=7.2 GPa, and Poisson's ratio ν=0.28. The fracture toughness K_{IC} of K9 optical glass was taken as 0.8 MPa m$^{1/2}$.

Table 2 Machining variables and their values for obtaining *K*

Experiment	Spindle speed (rpm)	Feed rate (mm/min)	Cutting depth (μm)	Cutting width (mm)	Ultrasonic amplitude (μm)
1st group	2,000, 3,000, 6,000	6	60	10	15
2nd group	3,000	2, 6, 12	60	10	15
3rd group	3,000	6	30, 60, 80	10	15

As assumed in the development of the model, the proportionality constant *K* is independent of input variables. Therefore, only one experiment can obtain the value of *K*. To verify that it is indeed independent of input variables, many experiments with different input variables were conducted. The design of experiments is given in Table 2. The experiments involve three groups of input variables (spindle speed, feed rate, and cutting depth). The resonance frequency for the selected diamond cutter with the ultrasonic spindle was 17 kHz. To obtain better ultrasonic vibration characteristics, i.e., ultrasonic amplitude and power, the ultrasonic frequency was set at 17 kHz. The ultrasonic amplitude of the diamond cutter was 15 μm as measured with a laser fiber vibrometer (Polytec, Germany), and the ultrasonic power was 13 W. The same diamond cutter was used during all experiments. The abrasive concentration C_a was taken as 100.

4.3 Obtaining *K*

The value of *K* can be estimated using the results obtained from designed experiments. For each test, one value of *K* can be obtained using the measured cutting force and input variables. In this study, the apex angle of the abrasive grain α_0, abrasive concentration C_a, abrasive size S_a, and the geometrical factor of indenter were taken as 90°, 170, 90 μm, and 1.85, respectively.

Figure 4 presents the values of *K* obtained from each experimental test. It is seen that the relationships between the values of *K* and input variables are not very relevant. Therefore, it can be reported that the assumption of *K* as a constant for certain conditions is feasible. The value of *K* can be used to estimate the cutting force for a given material under a range of input variables.

5 Model predictions and experimental verifications

In the section on obtaining *K*, designed experiments were conducted. To verify the developed mathematical model for the cutting force, experimental tests with an expanded range of input variables are performed in this section. Before the verification tests were carried out, the effects of individual

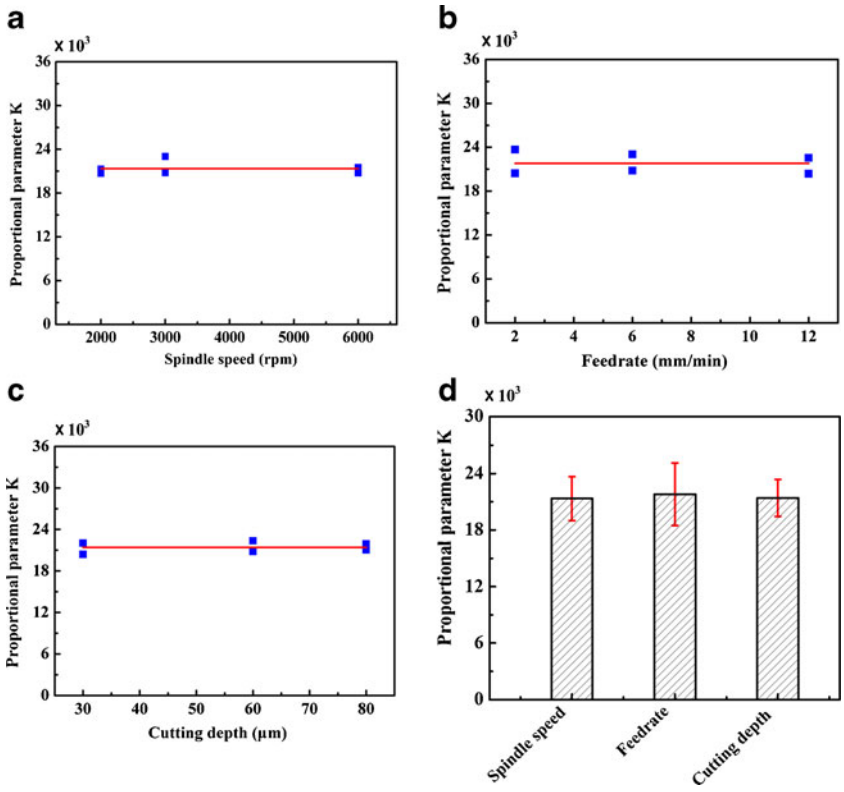

Fig. 4 Effects of input variables on *K*

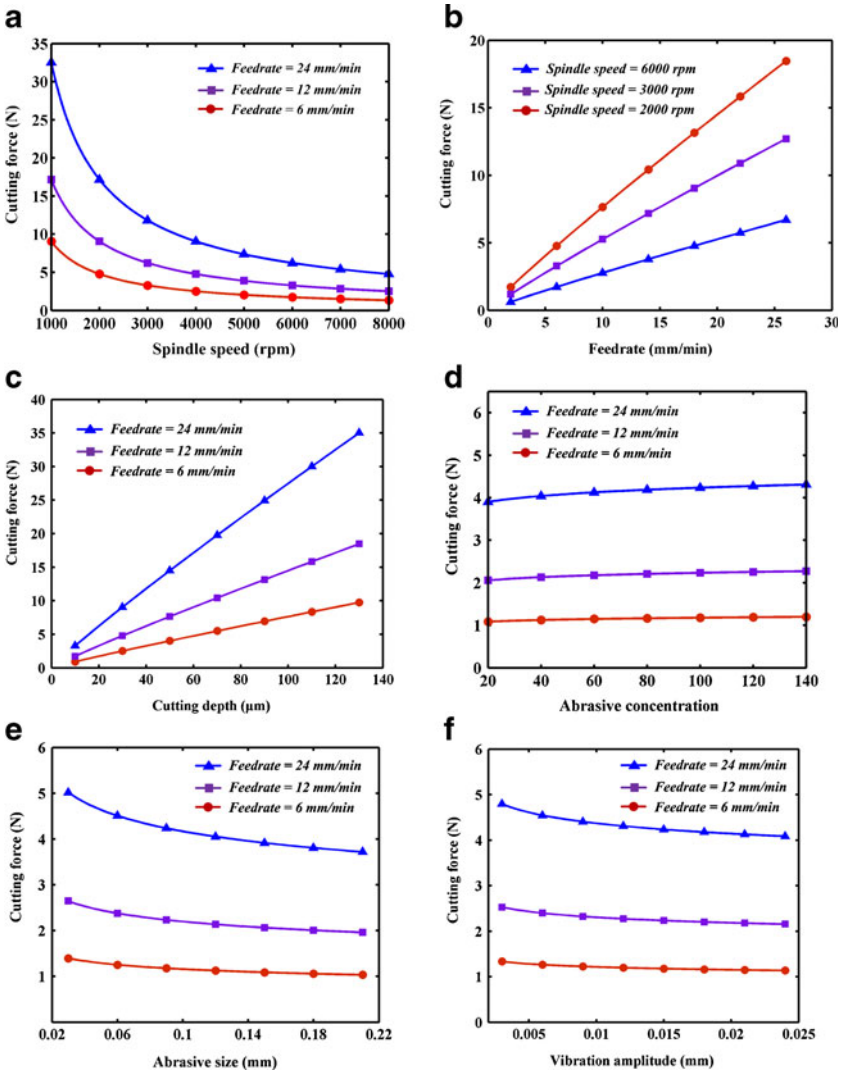

Fig. 5 Predicted relationships between cutting forces and input variables

input variables on the cutting force were determined using the established model. The value of K was taken as 21,520. Figure 5 shows the predicted relationships between cutting force and input variables. These figures show that the cutting force decreases as the spindle speed, ultrasonic vibration amplitude, and abrasive size increase, and increases with an increase in the feed rate, cutting depth, and abrasive concentration. Moreover, it is interesting that the cutting force varies slightly with a change in ultrasonic vibration amplitude, abrasive concentration, and abrasive size but varies strongly with a change in spindle speed, feed rate, and cutting depth. Therefore, it can be reported that the spindle speed, feed rate, and cutting depth notably affect the cutting force in the RUFM of brittle materials, and the ultrasonic vibration amplitude, abrasive concentration, and abrasive size have less affect on the cutting force.

The experimental setup for verification tests is the same as that presented in Section 4. The input variables and their values for verification tests are listed in Table 3. During the experiments, each variable was changed for six levels while keeping other variables constant.

Figure 6 shows the experimental and predicted results of the cutting force. Experimental results show that the cutting force decreases nonlinearly with an increase in spindle speed, and increases mostly linearly as the feed rate and cutting depth increase. Comparison of the cutting force between predicted results and experimental results shows that the trends of the predicted effects of the spindle speed, feed rate, and cutting depth are well consistent with the trends obtained from the experimental tests. Therefore, it is

Table 3 Machining conditions for verification tests

Variable	Unit	Value
Spindle speed	rpm	1,000, 2,000, 4,000, 5,000, 6,000, 8,000
Feed rate	mm/min	2, 6, 8, 12, 16, 24
Cutting depth	μm	10, 20, 30, 60, 80, 120

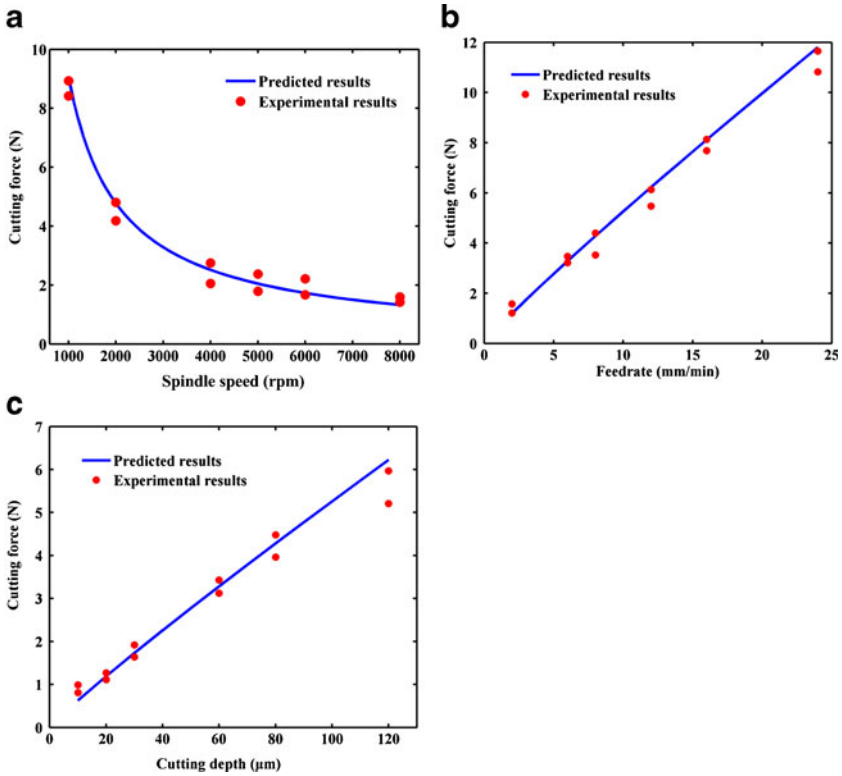

Fig. 6 Comparison of cutting force between predicted results and experimental results. **a** Feed rate=6 mm/min, cutting depth=60 μm; **b** spindle speed=3,000 rpm, cutting depth=60 μm; **c** spindle speed=3,000 rpm, feed rate=6 mm/min

concluded that the developed cutting force model can be applied to evaluate the cutting force for a given material.

6 Conclusions

A mathematical model for the cutting force in the RUFM of brittle materials was developed in this study. The developed cutting force model was experimentally verified in pilot experiments, and the cutting force was compared between predicted results and experimental results. The following conclusions are drawn from this study:

1. The developed model shows that the spindle speed, feed rate, cutting depth, ultrasonic vibration amplitude, abrasive concentration, abrasive size, and apex angle of the abrasive grain affect the cutting force. The predicted trends of the effects of input variables on the cutting force can be obtained from the developed cutting force model that the cutting force will decrease with an increase in the spindle speed, ultrasonic vibration amplitude, and abrasive size, and will increase as the feed rate, cutting depth, abrasive concentration, and apex angle of the abrasive grain increase.
2. Comparing the cutting force between predicted results and experimental results shows that the trends of predicted effects of input variables on the cutting force are well consistent with the trends obtained from the experiments. Therefore, the developed cutting force model can be applied to evaluate the cutting force in the RUFM of brittle materials.

Furthermore, the developing process of the cutting force model can be referred to establish the surface roughness prediction model in RUFM of brittle materials. It also can serve as a useful springboard for the development of model to predict the induced subsurface damage according the cracks generation and expansion mechanism of brittle materials in RUFM process. In addition, the modeling process of cutting force can be used for the development of cutting force model for changing feed axis to drilling in RUM of brittle materials.

Acknowledgments This research was financially supported by the National Natural Science Foundation of China (grant no. 50975153) and the State Key Laboratory of Tribology Foundation of China (grant no. SKLT11C7).

References

1. Arif M, Rahman M, Yoke San W (2011) Analytical model to determine the critical feed per edge for ductile–brittle transition in milling process of brittle materials. Int J Mach Tool Manuf 51(3):170–181
2. Pei ZJ, Ferreira PM, Haselkorn M (1995) Plastic flow in rotary ultrasonic machining of ceramics. J Mater Process Technol 48(1–4):771–777

3. Sayuti M, Sarhan Ahmed AD, Fadzil M, Hamdi M (2012) Enhancement and verification of a machined surface quality for glass milling operation using CBN grinding tool–Taguchi approach. Int J Adv Manuf Technol 60(9–12):939–950
4. Wan ZP, Tang Y (2009) Brittle–ductile mode cutting of glass based on controlling cracks initiation and propagation. Int J Adv Manuf Technol 43(11–12):1051–1059
5. Zhou M, Ngoi BKA, Yusoff MN, Wang XJ (2006) Tool wear and surface finish in diamond cutting of optical glass. J Mater Process Technol 174(1–3):29–33
6. Fang FZ, Chen LJ (2000) Ultra-precision cutting for ZKN7 glass. CIRP Ann Manuf Technol 49(1):17–20
7. Gu WB, Yao ZQ, Li HL (2011) Investigation of grinding modes in horizontal surface grinding of optical glass BK7. J Mater Process Technol 211(10):1629–1636
8. Chen ST, Jiang ZH, Wu YY, Yang HY (2011) Development of a grinding–drilling technique for holing optical grade glass. Int J Mach Tool Manuf 51(2):95–103
9. Belkhir N, Bouzid D, Herold V (2009) Surface behavior during abrasive grain action in the glass lapping process. Appl Surf Sci 255(18):7951–7958
10. Stephenson DJ, Sun X, Zervos C (2006) A study on ELID ultra precision grinding of optical glass with acoustic emission. Int J Mach Tool Manuf 46(10):1053–1063
11. Matsumura T, Muramatsu T, Fueki S (2011) Abrasive water jet machining of glass with stagnation effect. CIRP Ann Manuf Technol 60(1):355–358
12. Nath C, Lim GC, Zheng HY (2012) Influence of the material removal mechanisms on hole integrity in ultrasonic machining of structural ceramics. Ultrasonics 52(5):605–613
13. Kumar J, Khamba JS, Mohapatra SK (2009) Investigating and modeling tool-wear rate in the ultrasonic machining of titanium. Int J Adv Manuf Technol 41(11–12):1107–1117
14. Gan J, Wang X, Zhou M, Ngoi B, Zhong Z (2003) Ultraprecision diamond turning of glass with ultrasonic vibration. Int J Adv Manuf Technol 21(12):952–955
15. Liu K, Li XP, Rahman M, Liu XD (2004) Study of ductile mode cutting in grooving of tungsten carbide with and without ultrasonic vibration assistance. Int J Adv Manuf Technol 24(5–6):389–394
16. Liu K, Li XP, Rahman M (2008) Characteristics of ultrasonic vibration-assisted ductile mode cutting of tungsten carbide. Int J Adv Manuf Technol 35(7–8):833–841
17. Peng Y, Wu YB, Liang ZQ, Guo YB, Lin X (2011) An experimental study of ultrasonic vibration-assisted grinding of polysilicon using two-dimensional vertical workpiece vibration. Int J Adv Manuf Technol 54(9–12):941–947
18. Yan Y, Zhao B, Liu J (2009) Ultraprecision surface finishing of nano-ZrO2 ceramics using two-dimensional ultrasonic assisted grinding. Int J Adv Manuf Technol 43(5–6):462–467
19. Peng Y, Liang Z, Wu Y, Guo Y, Wang C (2012) Characteristics of chip generation by vertical elliptic ultrasonic vibration-assisted grinding of brittle materials. Int J Adv Manuf Technol 62(5–8):563–568
20. Shen XH, Zhang JH, Xing DL, Zhao YF (2012) A study of surface roughness variation in ultrasonic vibration-assisted milling. Int J Adv Manuf Technol 58(5–8):553–561
21. Shen XH, Zhang JH, Li H, Wang JJ, Wang XC (2012) Ultrasonic vibration-assisted milling of aluminum alloy. Int J Adv Manuf Technol 63(1–4):41–49
22. Pei ZJ, Prabhakar D, Ferreira PM, Haselkorn M (1995) Mechanistic approach to the prediction of material removal rates in rotary ultrasonic machining. J Eng Ind 117(2):142–151
23. Gong H, Fang FZ, Hu XT (2010) Kinematic view of tool life in rotary ultrasonic side milling of hard and brittle materials. Int J Mach Tool Manuf 50(3):303–307
24. Lv DX, Huang YH, Tang YJ, Wang HX (2012) Relationship between subsurface damage and surface roughness of glass BK7 in rotary ultrasonic machining and conventional grinding processes. International Journal of Advanced Manufacturing Technology. doi:10.1007/s00170-012-4509-1
25. Li ZC, Jiao Y, Deines TW, Pei ZJ, Treadwell C (2005) Rotary ultrasonic machining of ceramic matrix composites: feasibility study and designed experiments. Int J Mach Tool Manuf 45(12–13):1402–1411
26. Zhang CL, Feng PF, Zhang JF, Wu ZJ, Yu DW (2012) Investigation into the rotary ultrasonic face milling of K9 glass with mechanism study of material removal. Int J Manuf Technol Manag 25(4):248–266
27. Cong WL, Feng Q, Pei ZJ, Deines TW, Treadwell C (2012) Edge chipping in rotary ultrasonic machining of silicon. Int J Manuf Res 7(3):311–329
28. Zhang CL, Feng PF, Zhang JF (2013) Ultrasonic vibration-assisted scratch-induced characteristics of C-plane sapphire with a spherical indenter. Int J Mach Tool Manuf 64(1):38–48
29. Ya G, Qin HW, Yang SC, Xu YW (2002) Analysis of the rotary ultrasonic machining mechanism. J Mater Process Technol 129(1–3):182–185
30. Zhang QH, Wu CL, Sun JL, Jia ZX (2000) Mechanism of material removal in ultrasonic drilling of engineering ceramics. Proc Inst Mech Eng B J Eng Manuf 214(9):805–810
31. Liu DF, Cong WL, Pei ZJ, Tang YJ (2012) A cutting force model for rotary ultrasonic machining of brittle materials. Int J Mach Tool Manuf 52(1):77–84
32. Zhang CL, Feng PF, Wu ZJ, Yu DW (2011) Mathematical modeling and experimental research for cutting force in rotary ultrasonic drilling. Chin J Mech Eng 47(15):149–155
33. Singh R, Khamba JS (2009) Mathematical modeling of tool wear rate in ultrasonic machining of titanium. Int J Adv Manuf Technol 43(5–6):573–580
34. Kumar J, Khamba JS (2010) Modeling the material removal rate in ultrasonic machining of titanium using dimensional analysis. Int J Adv Manuf Technol 48(1–4):103–119
35. Pei ZJ, Ferreira PM, Kapoor SG, Haselkorn M (1995) Rotary ultrasonic machining for face milling of ceramics. Int J Mach Tool Manuf 35(7):1033–1046
36. Pei ZJ, Ferreira PM (1999) Experimental investigation of rotary ultrasonic face milling. Int J Mach Tool Manuf 39(8):327–1344
37. Turchetta S (2009) Cutting force on a diamond grit in stone machining. Int J Adv Manuf Technol 44(9–10):854–861
38. Patnaik Durgumahanti US, Singh V, Venkateswara Rao P (2010) A new model for grinding force prediction and analysis. Int J Mach Tool Manuf 50(3):231–240
39. Fang FZ, Zhang GX (2004) An experimental study of optical glass machining. Int J Adv Manuf Technol 23(3):155–160
40. Arif M, Rahman M, San W, Doshi N (2011) An experimental approach to study the capability of end-milling for microcutting of glass. Int J Adv Manuf Technol 53(9):1063–1073
41. Jiao F (2008) The Theoretical and experimental studies on ultrasonic aided high efficiency lapping with solid abrasive of engineering ceramic, Ph. D. thesis. Shanghai Jiao Tong University
42. Marshall DB, Lawn BR, Evans AG (1982) Elastic/plastic indentation damage in ceramics: the lateral crack system. J Am Ceram Soc 65(11):561–566